S6

MOLECULAR SIMULATIONS OF ZN-AL LAYERED DOUBLE HYDROXIDE INTERCALATED WITH PORPHYRIN ANIONS

P. Kovář[1], M. Pospíšil[1], K. Lang[2]

[1]*Charles University in Prague, Faculty of Mathematics and Physics, Ke Karlovu 3, 121 16 Prague, Czech Rebublic*

[2]*Institute of Inorganic Chemistry, v.v.i., Academy of Sciences of the Czech Republic, Řež 250 68, Czech Republic*

Kovar@karlov.mff.cuni.cz

Layered Double Hydroxides (LDHs) belong to the inorganic layered solids consisted of the rigid layers containing two kinds of metallic atoms and the interlayers containing exchangeable compensating anions and water molecules. These materials are attractive due to their simple modification and they are used in many branches like catalysis, precursors for chemical reactions, drug delivery, decontamination of water, soils, etc. The intercalation of porphyrins into Layered Double Hydroxides based on ion exchange plays an important role in designing of new materials with optical properties, which can be used as photofunctional units [1]. Advanced methods of preparation of the sample allow us to obtain well crystallized samples and their structure analysis can provide deeper structural details. Zn(II)-5,10,15,20-tetrakis(4-sulfonatophenyl) porphyrin – (ZnTPPS) shown in Fig. 1 was intercalated into Zn_2-Al LDH and a high crystallinity was achieved by the coprecipitation procedures followed by a post-synthesis hydrothermal treatment.

Molecular simulations and quantum chemistry calculations combined with X-ray diffraction, thermogravimetry and electron density measurements were used in the structure analysis. The geometry and dimensions of ZnTPPS were optimized by the quantum-chemistry computational program Turbomole v5.9 using the RI-DFT method with B-P86 functional [2]. The optimized models of porphyrins were subsequently used in the molecular simulations. The cell parameters were determined from experimental XRD patterns: $a = b = 3.064$ Å. 96 cells were linked to obtain the layer $[Zn_{64}Al_{32}(OH)_{192}]^{32+}$ with the lattice parameters: A = 49.024 Å and B = 18.384 Å. The basal spacing in initial models was equal to the value of the experimental basal spacing (23.05 Å) obtained from the experimental XRD data. The estimated loading of ZnTPPS anions in the interlayer space was over 90% of anion exchange capacity (AEC). It was approximated by structural models with the 100% loading of AEC. The initial models contained 4 water molecules *per* $[Zn_4Al_2(OH)_{12}]^{2+}$. The composition of initial structure models was $[Zn_{192}Al_{96}(OH)_{576}]$ $[(ZnTPPS)_{24}\cdot 192\ H_2O]$ and a set of models with various orientations of guest anions with respect to the host layers and with respect to each other was created. The minimization of the initial models was carried out in the Universal force field [3], the electrostatic energy was calculated by Ewald summation method [4] and the van der Waals energy was calculated by Lennard-Jones potential [5]. The space group was P1 and the porphyrin pyrroles were kept in their geometry as it was obtained by ab-initio

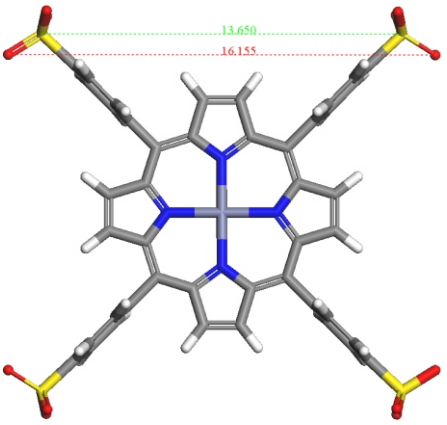

Figure 1. Molecular structure of ZnTPPS and its dimensions.

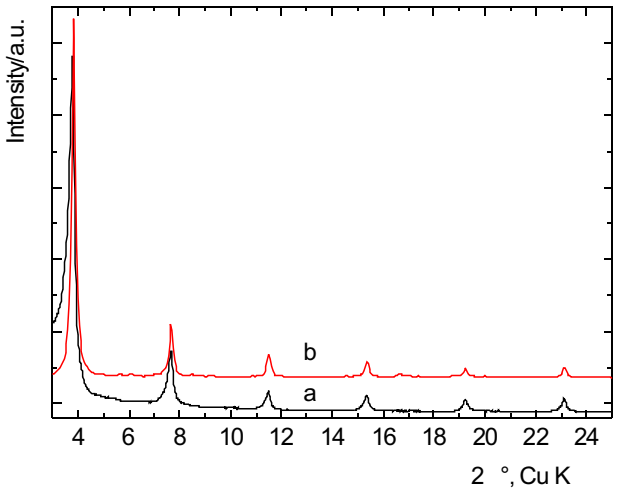

Figure 2. Experimental (a) and calculated (b) XRD basal diffractions of Zn_2Al/ZnTPPS intercalate.

calculations. The models were minimized iteratively in two steps, with fixed and variable cell parameters to obtain a good estimation of the orientation of the guest with respect to the host layers and a good agreement with the experimental basal spacing. The minimized models were refined by quench dynamics in an NVT (constant number of atoms, constant volume and constant temperature) statistical ensemble at a temperature of 300 K. One dynamics step was 0.001 ps and 200 ps of dynamics were carried out.

The results are summarized in Figs. 2 and 3. Fig. 2 shows the calculated and experimental powder XRD patterns with basal diffraction lines characterizing the interlayer arrangement and are compared for *2* from 3 to 25°. The arrangement of the guests in the interlayer space corresponding to the calculated powder XRD pattern is shown in Fig. 3. The porphyrin anions are horizontally shifted, the horizontal shift ranges from one third to one half of the porphyrin diameter and the guests nearly homogeneously occupy the interlayer space. The low intensity peaks in the calculated XRD especially between 5 and 6° and between 16 and 18° are caused by the forced periodicity of central zinc atoms of ZnTPPS. It indicates that in the real sample one can expect no order of the guests in the interlayer space. The ZnTPPS porphyrin planes exhibit a Åtilted orientation with respect to the normal. The average calculated value of tilted angle is of 14°.

1. K. Lang, P. Bezdička, J.L. Bourleande, J. Hernando, I. Jirka, E. Káfuňková, F. Kovanda, P. Kubát, J. Mosinger, D.M. Wágnerová, *Chem. Mater.,* **19**, (2007), 3822.
2. R. Ahlrichs, M. Bär, M. Häser, H. Horn, C. Kölmel, *Chem. Phys. Lett.,* **162,** (1989), 165.
3. A.K. Rappé, C.J. Casewit, K.S. Colwell, W.A. Goddard III, W.M. Skiff, *J. Am. Chem. Soc.,* **114,** (1992), 10024.
4. N. Karasawa, W.A. Goddard, *J. Phys. Chem.,* **93,** (1989), 7320.

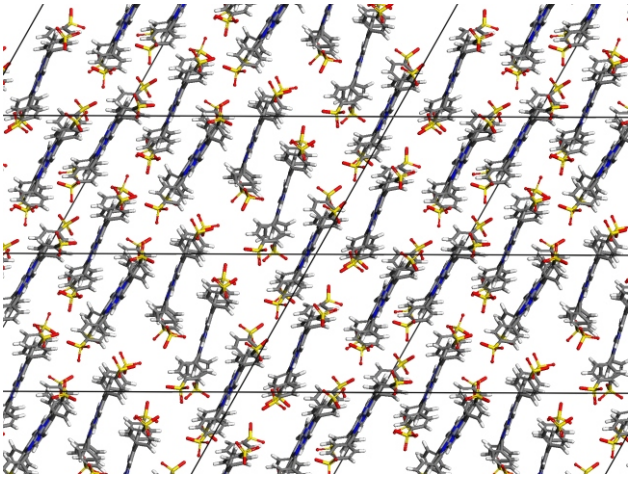

Figure 3. Top view of the linked supercells on the arrangement of the guests in the interlayer space.

5. J.E. Lennard-Jones, *Proc. Royal Soc. of London,* **109,** (1925), 584.

Acknowledgements

The work was supported by GAČR 205/08/0869 and by MSM 0021620835.

S7

HIGH-RESOLUTION STRUCTURE OF EXTRACELLULAR DOMAIN OF HUMAN CD69

P. Kolenko[1,2], O. Vaněk[3], T. Skálová[2], J. Dohnálek[2], J. Dušková[2], A. Štěpánková, K. Bezouška[3], J. Hašek[2]

[1]Dept. of Solid State Engineering, FNSPE CTU, Trojanova 13, 120 00 Praha 2
[2]Institute of Macromolecular Chemistry AS CR, Heyrovského nám. 2, 162 06 Praha 6
[3]Dept. of Biochem., Faculty of Science, Charles University in Prague, Hlavova 8, 12840 Praha 2
kolenko@imc.cas.cz

Natural killer cells a are part of our innate immune defense able to kill several types of tumor cells. Their activity is regulated by activation or inhibition signals coming from receptors expressed on cell surface. Studies of these receptors provide novel insights into the mechanisms of function of natural killer cells.

The extracellular domain of human CD69 was crystallized using novel polymer screens [1]. The crystals belonging to space group $P6_1$ diffracted to high resolution (1.37) and were merohedrally twinned. The structure provides the most detailed information on intra- and intermolecular interactions of the human CD69 receptor. A comparative analysis of CD69 including homologous structures is performed.

CD69 belongs to the earliest induced cell surface glycoproteins during natural killer cell activation. Recombinant forms of the extracellular part of the receptor can be potentially used in cancer treatment. However, the mechanism of function of the molecules still remains unclear in spite of the fact that many biochemical and biophysical studies were reported [2].

This work was supported by GA AV IAA500500701, GA ČR 305/07/1073 and European Commission Integrated project SPINE2-Complexes, no. 031220.

1. J. Hašek, J. Dohnálek, J. Dušková, T. Skálová, P. Kolenko, T. Koval, A. Štěpánková, *Acta Cryst.*, A**64,** (2008), C233.
2. O. Vaněk et al., *FEBS Journal*, **275**, (2008), 5589.

S8

CRYSTAL STRUCTURE OF THE RECEIVER DOMAIN OF THE HISTIDINE KINASE CKI1 FROM *Arabidopsis thaliana*

T. Klumpler, B. Pekárová, J. Marek, P. Borkovcová, L. Janda, J. Hejátko

Laboratory of Molecular Plant Physiology, Department of Functional Genomics and Proteomics, Institute of Experimental Biology, Faculty of Science, Masaryk University
klumpler@sci.muni.cz

The crystal structure of the receiver domain of the histidine kinase CKI1 from *Arabidopsis thaliana* has been determined at a resolution of 2.0 Å.

Sensor histidine kinases (HKs) are members of the two-component (TC) signalling systems that mediate signal transduction in a broad spectrum of adaptive responses in bacteria [1]. A modified version of bacterial two-component (TC) signalling has been adapted by yeast and plants. In TC signalling in plants, the membrane-associated sensor HK interacts with a signalling molecule, which activates an intracellular HK domain and leads to autophosphorylation of its conserved histidine moiety. The downstream phosphorelay is initiated by a receiver domain (RD) of the HK. The RD transfers phosphate from a His to its own Asp and further transmits the signal via transphosphorylation to the His of a histidine-containing phosphotransfer (HPt) domain. The HPt proteins translocate the signal to the nucleus, where the phosphorylated histidine serves as a donor for the phosphorylation of a final phosphate acceptor, the Asp residue of the response regulator [2].

In the *A. thaliana* genome, genes encoding 11 HKs, 6 HPt proteins and 23 response regulators have been identified. *A. thaliana* HKs mediate discrete responses to various phytohormones (ethylene, cytokinin and abscisic acid) and osmosensing [3]. This suggests that the structure of the RD might contribute to the recognition of its interaction partners.

The sensor histidine kinase CKI1 was identified as an activator of a cytokinin-like response when overexpressed in hypocotyl explants of *A. thaliana* [4]. However, in contrast to the genuine cytokinin receptors of *A. thaliana*, AHK2, AHK3 and AHK4, CKI1 was found to be constitutively active in bacteria and yeast or *A. thaliana* protoplasts [5-6]. Thus, the specificity and the role of CKI1 in the TC signalling in *A. thaliana* remain unclear.

Crystals of the recombinant RD of the *Arabidopsis* HK CYTOKININ-INDEPENDENT1 ($CKI1_{RD}$) have been obtained by the hanging-drop vapour-diffusion method using ammonium sulfate as a precipitant and glycerol as a cryoprotectant. The crystals diffracted at beamline BW7B of the DORIS-III storage ring to approx. 2.4 Å. The diffraction has been improved significantly - to at least 2.0 ÅĹ - after applying of a non-water cryoprotectant. The crystals belong to space group $C222_1$ with unit-cell parameters a = 54.46, b = 99.82, c = 79.94 Å, the asymmetric unit contains one molecule of the protein. The structure of $CKI1_{RD}$ had been solved by a molecular-replacement method using an automated scheme for molecular replacement as implemented in MrBUMP v.0.4.1 in conjunction REFMAC as the refinement program. An unambiguous solution was found using the bacterial response-regulator protein CheY [7] as a search model. Initial R value of 0.54, which decreased to R = 0.413 and Rfree = 0.426 after 30 cycles of REFMAC refinement. The quality of the map generated with this result was good enough to allow successful application of the autobuild regime of ARP/wARP.

The three-dimensional structure of *A. thaliana* $CKI1_{RD}$ shows the conformational conservation of receiver proteins, such as CheY, CheB, ETR_{RD}. $CKI1_{RD}$ is a single domain protein folded in a ( )$_5$ manner with a central -sheet formed from five -strands and surrounded by sides by two and three -helices. The catalytic aspartate residue is located on the carboxyl terminus of the central 3-strand, in a cavity formed by loops L1, L5 and L7 loops. All major conformational differences between receiver proteins are located in the loops, which supposedly form a docking interface for the ineracting partners.

1. E. Calva, R. Oropeza, *Microb. Ecol.,* **51**, (2006), 166-176.
2. J. P. To, J. J. Kieber, *Trends Plant Sci*., **13**, (2008), 85-92.
3. T. Mizuno, Biosci. *Biotechnol. Biochem*. **69**, (2005), 2263–2276.
4. T. Kakimoto, *Science*, **274**, (1996), 982–985.
5. H. Yamada, T. Suzuki, K. Terada, K. Takei, K. Ishikawa, K. Miwa, T. Yamashino, T. Mizuno, *Plant Cell Physiol*., **42**, (2001), 1017–1023.
6. I. Hwang, J. Sheen, *Nature (London),* **413**, (2001), 383–389.
7. D. Wilcock, M. T. Pisabarro, E. Lopez-Hernandez, L. Serrano, M. Coll, *Acta Cryst. D.,* **54**, (1998), 378–385.

S9

DRUG DESIGN OF SELECTIVE 5'-NUCLEOTIDASES INHIBITORS

Petr Pachl[1], Jiří Brynda[1,2], Ivan Rosenberg [2], Milan Fábry[1], Pavlína Řezáčová[1,2,]

[1]Institute of Molecular Genetics, Flemingovo nam. 2, Prague 6, Prague, 16610, Czech Republic,
[2]Institute of Organic Chemistry and Biochemistry AS CR, Flemingovo nam. 2, Prague 6, Prague, 16610, Czech Republic, petr.pachl@img.cas.cz

The monophosphate 5'-nucleotidases, including 5'(3')-deoxyribonucleotidase, belong to a family of enzymes that catalyze the dephosphorylation of nucleoside monophosphates. The ribonucleotides and deoxyribonucleotides could be synthesized *de novo* from low-molecular-weight precursors or by salvage from nucleosides or nucleobases coming from catabolism of nucleic acids [1]. In this salvage pathway, ribonucleotides and deoxyribonucleotides are phosphorylated by nucleoside and nucleotide kinases to maintain sufficient pools of dNTP's and NTP's for synthesis of DNA and RNA. The phosphorylation by cellular nucleoside kinases is opposed by 5'-nucleotidases that dephosphorylate ribo- and deoxyribonucleoside monophosphates [2, 3, 4]. Besides their role in the regulation of physiological dNTP pools, substrate cycles between ribonucleotidases and kinases may affect the therapeutic action of pyrimidine nucleoside analogs used as anticancer and antiviral agents. Such compounds require the nucleoside kinases activity for phosphorylation to their active forms. Results of clinical and *in vitro* studies propose that an increase in nucleotidase activity can interfere with nucleoside analogue activation resulting in drug resistance [5].

The main goal of this project is the search for potent and selective inhibitors of mammalian 5'-nucleotidases based on nucleoside phosphonic acids and their derivatives and comparison of sensitivity of 5'-nucleotidases isolated from various sources toward individual inhibitors.

We have prepared 2 types of human 5'-nucleotidase: cytosolic and mitochondrial by recombinant expression in *E. coli*. The inhibitory properties of a series of nucleoside phosphonic acids derivatives are tested and for the most promising compounds the enzyme-inhibitor structure will be determined to serve as a lead for structure-based drug design efforts.

In general, compounds of strong and selective inhibitory potency are of high medicinal interest as antimetabolites for anticancer and antiviral therapy.

1. P. Reichard: Interactions between deoxyribonucleotide and DNA synthesis. *Annu Rev Biochem.,* 57 (1988), 349-74.
2. S.A. Hunsucker, B.S. Mitchell, J. Spychala: The 5'-nucleotidases as regulators of nucleotide and drug metabolism. *Pharmacol Ther*., 107 (2005), 1-30.
3. V. Bianchi, E. Pontis, P. Reichard: Interrelations between substrate cycles and de novo synthesis of pyrimidine deoxyribonucleoside triphosphates in 3T6 cells. *Proc Natl Acad Sci U S A,* 83 (1986), 986-90.
4. P. Bianchi, E. Fermo, F. Alfinito, C. Vercellati, M. Baserga, F. Ferraro, I. Guzzo, B. Rotoli, A. Zanella: Molecular characterization of six unrelated Italian patients affected by pyrimidine 5'-nucleotidase deficiency. *Br J Haematol,* 122 (2003), 847-51.
5. C. Mazzon, C. Rampazzo, M.C. Scaini, L. Gallinaro, A. Karlsson, C. Meier, J. Balzarini, P. Reichard, V. Bianchi: Cytosolic and mitochondrial deoxyribonucleotidases: activity with substrate analogs, inhibitors and implications for therapy. *Biochem Pharmacol,* 66 (2003), 471-9.

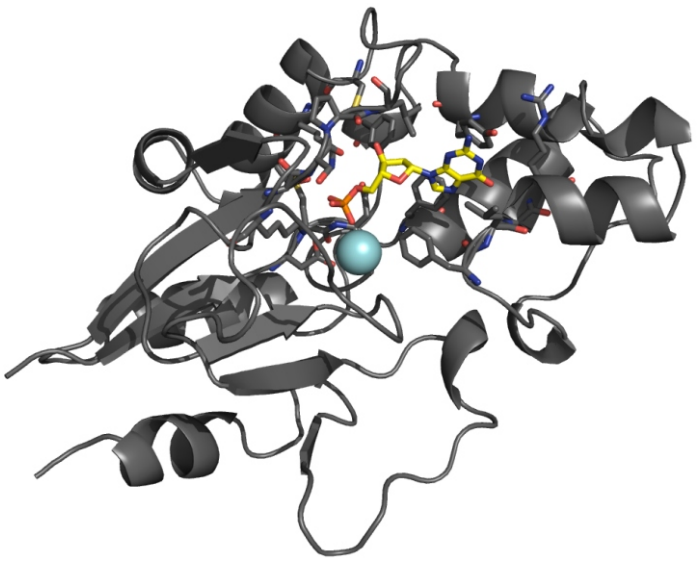

Figure 1. X-ray structure structure of human cytosolic 5'-nucleotidase with catalytic magnesium ion represented as a cyan sphere and modeled dGMP shown in stick model with yellow carbon atoms.

S10

INTERACTIONS BETWEEN THE ENZYME AND ITS LIGANDS IN THE ACTIVE SITE OF -GALACTOSIDASE

Andrea Štepánková[1, 2], Tereza Skálová[2], Jan Dohnálek[2], Jarmila Dušková[2], Petr Kolenko[1, 2], Jindrich Hašek[2], Vojtech Spiwok[3], Petra Lipovová[3]

[1]Dept. of Solid State Physics, FNSPE, CTU, Trojanova 13, 120 00, Prague 2, Czech Republic
[2]Institute of Macromolecular Chemistry AS CR, v.v.i., Heyrovského nám. 2, 162 06, Prague 6, Czech Rep.
[3]Dept. of Biochemistry, ICT, Technická 5, 166 28, Prague 6, Czech Republic, Stepanko@imc.cas.cz

-Galactosidase (EC 3.2.1.23) is an enzyme which is able to catalyze hydrolysis of the terminal -D-galactosyl of -D-galactosides and it is also able to catalyze trans-glycosylation and belongs to the enzyme class called glycosidases.

Recently, we determined the structure of the wild type enzyme -galactosidase from *Arthrobacter* sp. C2-2 [1]. Structures of its complexes with -D-galactose, -D-galactonolactone and isopropyl -D-1-thiogalactopyranoside (IPTG) determined by X-ray diffraction are presented here. X-ray diffraction data were collected at the beam-line ID14.1 of the source of synchrotron radiation ESRF in Grenoble and on an in-house rotating anode diffractometer. The data were processed using HKL2000. All the three crystals belong to the same space group $P2_1$ but packing of hexamers in the crystals differs. The asymetric unit contains one hexamer with a molecular weight of 660 kDa.

This paper reviews the interactions between several type of ligands and the enzyme. Our structures of complexes of the enzyme from *Arthrobacter* sp. C2-2 are compared with a series of complexes of -galactosidase from *E. coli* [2].

There are two distinct binding modes for the galactosyl group of substrate - shallow and deep. Each binding mode has specific hydrogen bonds between enzyme and bound ligands. Structure changes evoked by binding of ligands into the active site of the enzyme will be shown and discussed. -D-galactose, as well as -D-galactonolactone, occupy the deep binding position and make the same interactions but large structure changes with regard to non-liganded enzyme are observed only in the case of -D-galactonolactone.

1. Skálová, T. et al.: Cold-active -galactosidase from *Arthrobacter* sp. C2-2 forms compact 660 kDa hexamers: Crystal structure at 1.9 Å resolution. *J. Mol. Biol.*, **353**, 282-294 (2005).
2. Juers D. H. et al.: A structural view of the action of *Escherichia coli (lacZ) -galactosidase, Biochemistry*, **40**, 14781-14794 (2001).

This work was supported by the Czech Science Foundation (305/07/1073) and by the IGS CTU (CTU0803914).

S11

CRYSTALLIZATION STUDY OF THE IRON-REGULATED OUTER MEMBRANE LIPOPROTEIN (FRPD) FROM *Neisseria meningitidis*

E. Sviridova[1], L. Bumba[2], P. Sebo[,3] and I. Kuta Smatanova[1,4]

[1]Institute of Physical Biology USB CB, Zamek 136, 373 33 Nove Hrady, Czech Republic
[2]Institute of Microbiology AS CR, Videnska 1083, 142 20 Prague, Czech Republic
[3]Institute of Biotechnology AS CR, Videnska 1083, 142 20 Prague, Czech Republic
[4]Institute of Systems Biology and Ecology AS CR, Zamek 136, 373 33 Nove Hrady, Czech Republic
sviridova@greentech.cz

Neisseria meningitidis is a Gram-negative bacterium colonizing the nasopharynx of about 10% of healthy humans. Occasionally the meningococci can traverse the mucosal epithelia to reach the bloodstream, eventually cross the blood-brain barrier, and cause rapidly progressing septicemia and/or meningitis [1]. Several traits potentially required for virulence of meningococci have been identified, including production of a capsule conferring resistance to serum, secretion of an IgA protease, the high antigenic variability of pili and non-fimbrial adhesins, and the presence of several iron acquisition systems [2]. Under conditions of limited iron availability, *N. meningitidis* produces Fe-regulated proteins, FrpD and FrpC. FrpC belongs to a family of type I-secreted RTX (Repeat in toxins) proteins and it may be involved in the pathogenesis of meningococcal infection. FrpD binds the N-terminal portion of FrpC with a very high affinity and probably serves as an accessory lipoprotein involved in anchoring of the secreted RTX protein to the outer bacterial membrane [3]. The aim of this project is to produce crystals of FrpD protein for X-ray diffraction experiments and to solve the structure of FrpD protein.

The recombinant, truncated version of the FrpD protein lacking the first 21 amino acid residues ($FrpD_{250}$) with the C-terminal polyhistidine tag, was expressed in *E. coli* BL21 DE3 and purified using a combination of metal affinity and anion-exchange column chromatography. The crystals of truncated FrpD protein lacking the first 42 amino acid residues were obtained using a sitting drop vapour diffusion method. Diffraction data were collected at the beamline MX BL14.1 of synchrotron BESSY (Berlin, Germany) at 100 K to the resolution of 2.27 Å.

Crystals of FrpD belong to the hexagonal space group *P* 62, with unit-cell parameters $a = b = 115.33$ Å, $c = 38.79$ Å and $= = 90°$ and $= 120°$. To determine the structure of the FrpD protein, phase problem has to be solved using single/multiple anomalous diffraction (SAD/MAD) experiment hence the crystallization of selenomethionine derivative FrpD protein is currently in progress.

1. M. Guibourdenche, E. A. Hoiby, J. Y. Riou, F. Varaine, C. Joguet and D. A Caugant, *Epidemiology and Infection*, **116**, (1996), 115-120.
2. Y. L.Tzeng, D. S. Stephens, *Microbes and Infection*, **2**, (2000), 687–700.
3. K. Prochazkova, R. Osicka, I. Linhartova, P. Halada, M. Sulc, and P. Sebo, *The Journal of Biological Chemistry*, **280**, (2005), 3251-3258.

This project was supported by grants MSM6007665808 and LC06010 (Ministry of Education of the Czech Republic), AVOZ60870520 (Academy of Sciences of the Czech Republic) and GACR 310/06/0720.

S12

INVESTIGATION OF BIOCHEMICAL STRUCTURE AND FUNCTIONS OF THE *E. coli* PROTEIN WrbA

I. Kishko [1, 2], I. Kutá Smatanová[1,2], J. Carey [3], R. Ettrich [1, 2]

[1]*Institute of Physical Biology, USB CB, 37333 Nove Hrady, Czech Republic*
[2]*Institute of Systems Biology and Ecology, AS CR, 37333 Nove Hrady, Czech Republic*
[3]*Department of Chemistry, Princeton University, Princeton, New Jersey 08544-1009, USA*
Kishko@greentech.cz

The structure of the E.coli flavoprotein WrbA previously showed it is structurally related to eukaryotic NADH:quinone oxidoreductases (Nqos)[1]. Those enzymes have many unusual kinetic properties and their physiological function is not clear [2, 3].

WrbA and Nqos can transfer two electrons at a time from NADH to quinone acceptors. The electron transfer kinetics can be observed spectrophotometrically under steady-state conditions [1, 4, 5]. This assay is used to measure the rates of WrbA electron transfer and to evaluate different compounds that might function as the true physiological electron donors or acceptors. For the co-crystallization experiments we used standard equipment for crystallization, and varied the conditions that were established in our group for the holo protein crystals.

The results of this work demonstrate unusual two-plateau behaviour on the substrate concentration-dependence plots for NADH or benzoquinone. The experiments show that WrbA activity increases upon addition of membrane-mimicking detergents, and they demonstrate the ability of the protein to inactivate reversibly by shifting temperature from 5 to 25 ^{o}C. These properties are similar for the Nqos but have not been explained. Microcrystals of WrbA protein were crystallized using the sitting-drop vapour-diffusion technique [6]. Future studies with WrbA have the aim to explain kinetic properties in molecular terms and to create crystal good quality for diffraction analysis.

1. Laskowsi MJ, Dreher KA, Gehring MA, Abel S, Gensler AL, Sussex IM. *Plant Physiology,* **128**, (2002), 578-90.
2. Grandori R, Carey J. *Protein Science,* **3**, (1994), 2185-93.
3. Yang W, Ni L, Somerville RL. *Proc Natl Acad Sci U S A*, **90**, (1993), 5796-800.
4. Hosoda S, Nakamura W, Hayashi K. *J. Biol. Chem*., **249**, (1974), 6416-23.
5. Noll G, Kozma E, Grandori R, Carey J, Schodl T, Hauska G, Daub J. *Langmuir*, **22**, (2006), 2378-83.
6. A. Ducruix & R. Giegé, *Crystallization of Nucleic Acids and Proteins: A Practical Approach,* 2nd ed. Oxford: Oxford University Press, (1999).

This project was supported by grants: LC06010 (Ministry of Education of the Czech Republic), kontakt ME09016 and GAJU 079/2008/P.

S13

STRUCTURAL CHANGES OF TETRAMERIC FLAVOPROTEIN WRBA UPON FLAVIN BINDING

J. Wolfová[1,2], J. Brynda[1,3], J. R. Mesters[4], R. Ettrich[1,2], J. Carey[5], I. Kutá Smatanová[1,2]

[1]Institute of Physical Biology, University of South Bohemia České Budějovice, Zámek 136, CZ-373 33 Nové Hrady, Czech Republic
[2]Institute of Systems Biology and Ecology, Academy of Science of the Czech Republic, Zámek 136,CZ-373 33 Nové Hrady, Czech Republic
[3]Institute of Molecular Genetics, Academy of Sciences of the Czech Republic, Flemingovo nám. 2, CZ-16637 Prague 6, Czech Republic
[4]Institute of Biochemistry, Center for Structural and Cell Biology in Medicine, University of Lübeck, Ratzeburger Allee 160, 23538 Lübeck, Germany
[5]Chemistry Department, Princeton University, Washington Rd and William St, Princeton, NJ 08544-1009, USA
julinka.w@tiscali.cz

Introduction

Protein WrbA from *Escherichia coli* studied in this work represents a widely distributed family of tetrameric flavoenzymes [1, 2]. Using flavin mononucleotide (FMN) like monomeric flavodoxins that transfer single electrons to protein partners but forming multimers and carrying out two-electron reduction of quinones [3, 4] like the FAD-dependent quinone oxidoreductases, WrbA was suggested to be a structural and functional linker between bacterial flavodoxins and eukaryotic NAD(P)H:quinone oxidoreductases [5].

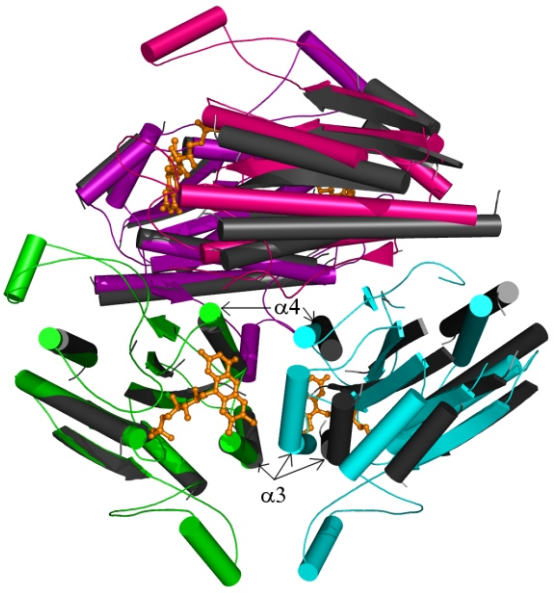

Figure 1. Overlay of holo- and apoWrbA tetramers. HoloWrbA subunits are green, cyan, pink and purple, all apoWrbA subunits are dark grey. helices are drawn as cylinders, strands as arrows, loops as lines. FMN cofactor in the holoWrbA structure is shown in ball and stick representation and colored orange. Larger distances between subunits across the empty FMN-binding site in apoWrbA tetramer bring the dark grey, cyan and pink subunits out of alignment, while the green and purple subunits of holoWrbA are aligned with the dark grey apoWrbA subunits nearly perfectly.

Interesting changes in protein dynamics and multimerization state accompanying FMN binding were identified by biophysical spectral methods [6]. This was motivation for the comparative analysis of the FMN-bound WrbA structure (holoWrbA) and the FMN-free WrbA structure (apoWrbA), results of which are presented here.

Materials and methods

Structures of holoWrbA and apoWrbA were solved from x-ray diffraction data on single crystals and refined to a resolution of 2.0 Å and 1.85 Å, respectively. Although crystals for both protein forms were grown from the same crystallization solution, different space groups were determined: $P4_12_12$ for holoWrbA and $P2_12_12$ for apoWrbA.

Results and discussion

In each structure four WrbA monomers form a tetramer, where individual subunits share the common fold of flavodoxins with sequence insertions unique for WrbA family forming additional secondary structure elements. FMN-binding sites are located at the interfaces of three of the four subunits. Our comparative analysis of holo- and apoWrbA revealed significant changes at the level of quaternary and tertiary structure. Large differences were observed in the arrangement of subunits in tetramers (see Fig. 1). In orthorhombic apoWrbA structure the distance between subunits across the empty FMN-binding site is larger by 2 to 4 Å than in holoWrbA structure, with the distances being longer at the surface than at the core of apoWrbA tetramer (see Fig. 2). Changes in structural organization of tetramers thought to be induced by FMN binding are in correspondence with the result of mass-spectrometry analysis [6] suggesting FMN to favour tetramer formation.

Substantial structural changes of WrbA monomers upon FMN binding are presumably located in the vicinity of the FMN-binding site. Structural overlay of holo- and apoWrbA monomers (see Fig. 3) shows the large relative motion of one of the loops contacting FMN in holoWrbA, resulting in partial occupation of the empty FMN-binding pocket in apoWrbA. FMN was also found to induce shifts

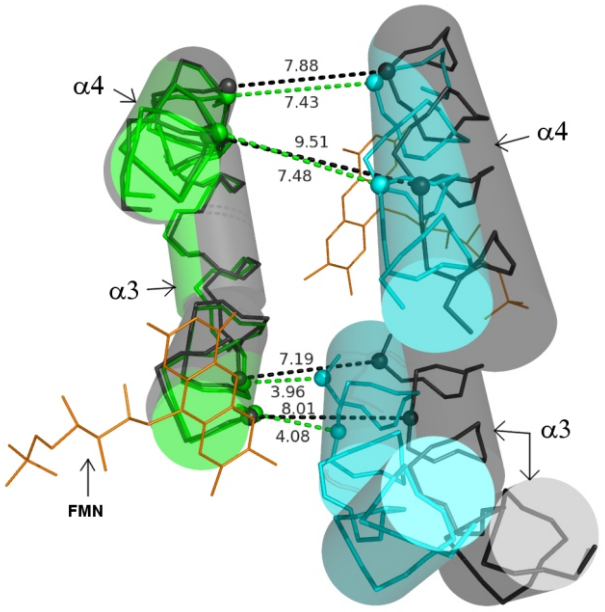

Figure 2. Interface between subunits formed across the FMN-binding site in holo- and apoWrbA tetramers. The detailed picture was drawn out of the overlay of WrbA tetramers shown in Fig. 1, thus colors and graphical representation are the same. Polypeptide main-chain atoms included in helices are shown in skeletal mode. Helices denoted as 3 and 4, labeled also in Fig. 1, were oriented to give an optimal view on the shift between subunits of apoWrbA relative to holoWrbA. Distances between the corresponding main-chain atoms (atoms shown as spheres) of the interfacing subunits are marked with dashed lines: green for holoWrbA, black for apoWrbA; their lengths measured in Ĺ indicate not only translational but also rotational shift of the subunits upon FMN binding.

in the positions of residues interacting with FMN, the most apparent being rotation of the side chain of Arg 78.

The 3D-superposition of holo- and apoWrbA with long-chain holo- and apoflavodoxin from *Anabaena* [7, 8] revealed striking similarities in the behavior of the FMN-binding residues in response to FMN binding, which are beyond those expectable from their distant homology. This finding indicates WrbA to be a significant member rather than a remote and unusual branch of flavodoxin-like proteins.

All figures included in this paper were prepared by using the PyMOL molecular graphic system [9].

1. R. Grandori & J. Carey, *Protein Sci.*, **3** (1994) 2185-2193.
2. R. Grandori, P. Khalifah, J.A. Boice, R. Fairman, K. Giovanelli & J. Carey, *J. Biol. Chem.*, **273** (1998) 20960-20966.
3. E.V. Patridge & J.G. Ferry, *J. Bacteriol.*, **188** (2006) 3498-3506.
4. G. Nöll, E. Kozma, R. Grandori, J. Carey, T. Schödl, G. Hauska & J. Daub, *Langmuir,* **22** (2006) 2378-2383.
5. J. Carey, J. Brynda, J. Wolfova, R. Grandori, T. Gustavsson, R. Ettrich & I. Kuta Smatanova, *Protein Sci.*, **16** (2006) 2301-2305.
6. A. Natalello, S.M. Doglia, J. Carey & R. Grandori, *Biochemistry*, **46** (2007) 543-553.
7. S.T. Rao, F. Shaffie, C. Yu, K.A. Satyshur, B.J. Stockman, J.L. Markley & M. Sundarlingham, *Protein Sci.*, **1** (1992) 1413-1427.
8. C.G. Genzor, A. Perales-Alcon, J. Sancho & A. Romero, *Nat. Struct. Biol.*, **3** (1996) 329-332.
9. W.L. DeLano: The PyMOL Molecuular Graphic System. San Carlos 2002. DeLano Scientific.

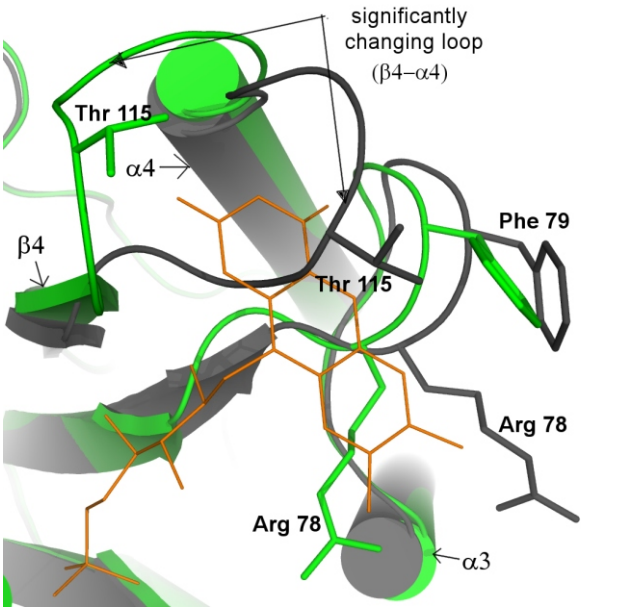

Figure 3. Overlay of holo- and apoWrbA monomers – detail of FMN-binding site. Colors and graphical representation are the same as in Fig. 1; holoWrba – green, apoWrbA – dark grey. Substantial changes accompanying FMN binding are indicated: 1) loop between 4 and 4 occupying partly the empty FMN-binding site in apoWrbA; 2) residues observed in different positions in holo- and apoWrbA are labeled and their side chains are shown as skeletal models. Selected secondary-structure elements are labeled.

This work was supported by the Ministry of Education of the Czech Republic (projects: Kontakt ME09016, MSM6007665808, LC06010) and by the Academy of Sciences of the Czech Republic (AV0Z60870520). Diffraction measurements at the synchrotron DESY/EMBL were supported by the European Community, Research Infrastructure Action under the FP6 "Structuring the European Research Area Specific Programme" to the EMBL Hamburg Outstation, Contract Number RII3-CT-2004-506008.

S14

STRUCTURAL CHARACTERIZATION OF THREE DHAA MUTANTS FROM *RHODOCOCCUS RHODOCHROUS*

A. Stsiapanava[1], J. Dohnalek[3], M. Kuty[1,2], J. A. Gavira[4], T. Koudelakova[5], J. Damborsky[5] and I. Kuta Smatanova[1,2]

[1]*Institute of Physical Biology University of South Bohemia Ceske Budejovice, Zamek 136, 373 33 Nove Hrady, Czech Republic*
[2]*Institute of Systems Biology and Ecology Academy of Science of the Czech Republic, Zamek 136, 373 33 Nove Hrady, Czech Republic*
[3]*Institute of Macromolecular Chemistry AS CR, Heyrovskeho nam.2, 162 00, Prague 6, Czech Republic*
[4]*Laboratorio de Estudios Cristalografico, Edificio BIC-Granada, Avda. de la Innovacion 1, P.T. Ciencias de la Salud, 18100-Armilla, Granada, Spain*
[5]*Loschmidt Laboratories, Faculty of Science, Masaryk University, Kamenice 5/A4, 62500 Brno, Czech Republic*
stepanova@greentech.cz

Haloalkane dehalogenases (EC 3.8.1.5) are members of the / -hydrolase fold family and catalyze hydrolytic conversion of a broad spectrum of hydrocarbons to the corresponding alcohols [1]. Besides a wide range of haloalkanes, DhaA can slowly convert serious industrial pollutant 1,2,3-trichloropropane (TCP) [2]. Three mutants marked as DhaA04, DhaA14 and DhaA15 were designed and constructed to study the relevance of the tunnels connecting the buried active site with the surrounding solvent for the enzymatic activity.

The three mutants of DhaA were crystallized using the sitting-drop vapor-diffusion technique [3]. Crystal growth conditions were optimized [4] and crystals were used for synchrotron diffraction measurements at the beamline X11 of the DORIS storage ring at the EMBL Hamburg Outstation. X-ray intensities data for DhaA04, DhaA14 and DhaA15 mutants were collected to a resolutions limit of 1.23 Å, 0.95 Å and 1.22 Å, respectively. Crystals of DhaA04 belong to the orthorhombic space group $P2_12_12_1$ while crystals of DhaA14 and DhaA15 mutants belong to the triclinic space group $P1$. The known structure of the haloalkane dehalogenase from *Rhodococcus* species (PDB code 1bn6) [5] was used as a template for the molecular replacement.

Analyses of crystal structures of mutants allow determine of electron densities observed for the ligands. In the case of DhaA04 the ligand is benzoic acid. DhaA14 and DhaA15 proteins contain isopropanol in the active site cavity. Mutations in Dha04 and DhaA15 partially block the main tunnel and almost completely block small slot in DhaA14 and DhaA15 enzymes.

1. D. B. Janssen, *Curr. Opin. Chem.l Biol.,* **8**, (2004), 150-159.
2. J. F. Schindler, P. A. Naranjo, D. A. Honaberger, C.-H. Chang, J. R. Brainard, L. A. Vanderberg, & C. J. Unkefer, *Biochemistry*, **38**, (1999), 5772–5778.
3. A. Ducruix & R. Giegé, *Crystallization of Nucleic Acids and Proteins: A Practical Approach,* 2nd ed. Oxford: Oxford University Press, (1999).
4 A. Stsiapanava, T. Koudelakova, M. Lapkouski, M. Pavlova, J. Damborsky & I. Kuta Smatanova, *Acta Cryst.* F**64**, (2008), 137-140.
5. J. Newman, T. S. Peat, R. Richard, L. Kan, P. E. Swanson, J. A. Affholter, I. H. Holmes, J. F. Schindler, C. J. Unkefer & T. C. Terwilliger, *Biochemistry,* **38,** (1999), 16105-16114.

The authors thank Jindrich Hasek (Academy of Sciences of the Czech Republic, Prague) and Juan Manuel Garcia-Ruiz (Laboratorio de Estudios Cristalografico, Edificio BIC-Granada) for their generous support. This work is supported by the Ministry of Education of the Czech Republic (MSM6007665808, LC06010) and the Academy of Sciences of the Czech Republic (AV0Z60870520). We are grateful to X11 Consortium for Protein Crystallography for access to their facility.